

# Observational constraints on cosmic strings: Bayesian analysis in a three dimensional parameter space

Levon Pogosian<sup>1</sup>, Mark Wyman<sup>2,3</sup>, and Ira Wasserman<sup>2,3</sup>

<sup>1</sup> *Institute of Cosmology, Department of Physics and Astronomy, Tufts University, Medford, MA 02155, USA*

<sup>2</sup> *Laboratory for Elementary Particle Physics, Cornell University, Ithaca, NY 14853, USA*

<sup>3</sup> *Center for Radiophysics and Space Research, Cornell University, Ithaca, NY 14853, USA*

(Dated: today)

Current data exclude cosmic strings as the primary source of primordial density fluctuations. However, in a wide class of inflationary models, strings can form at later stages of inflation and have potentially detectable observational signatures. We study the constraints from WMAP and SDSS data on the fraction of primordial fluctuations sourced by local cosmic strings. The Bayesian analysis presented in this brief report is restricted to the minimal number of parameters. Yet it is useful for two reasons. It confirms the results of [1] using an alternative statistical method. Secondly, it justifies the more costly multi-parameter analysis. Already, varying only three parameters – the spectral index and the amplitudes of the adiabatic and string contributions – we find that the upper bound on the cosmic string contribution is of order 10%. We expect that the full multi-parameter study, currently underway [2], will likely loosen this bound.

PACS numbers: 98.80.Cq

The idea that inflationary cosmology might lead to cosmic string formation is not new [3] and has received new impetus from brane inflation scenarios suggested by superstring theory [4, 5, 6, 7, 8, 9, 10]. In these models, inflation can arise during the collisions of branes that coalesce to form, ultimately, the brane on which we live [4, 11, 12, 13]. It is possible to build brane inflation models that predict adiabatic temperature and dark matter fluctuations capable of reproducing all currently available observations. A seemingly unavoidable outcome of brane inflation, however, is the production of a network of local cosmic strings [5, 6], whose effects on cosmological observables range from negligible to substantial, depending on the specific brane inflationary scenario [8, 9]. As the precision of cosmological observations increases, we might hope to be able to distinguish among numerous presently viable models of inflation by the properties of the cosmic strings they predict.

The fluctuations resulting from brane inflation are expected to be an incoherent superposition of contributions from adiabatic perturbations initiated by curvature fluctuations and active perturbations induced by the decaying cosmic string network. The resulting CMB temperature power spectrum can be written as

$$C_l = WC_l^{\text{adiabatic}} + BC_l^{\text{strings}}, \quad (1)$$

where  $W$  and  $B$  are weighting factors. Analogous expressions hold for matter density and polarization power spectra. In Eq. (1), the weight factors  $W$  and  $B$  determine the relative importance of the adiabatic and cosmic string contributions. We choose the weight factor  $W$  so that  $W = 1$  for the WMAP's best fit power law model [15] with no cosmic strings.

The scaling properties of the cosmic string networks in brane inflationary scenarios are different from those of

the more familiar 3+1 D field theoretical strings, since intercommutation probabilities are smaller as a consequence of the existence of extra dimensions [8, 9]. As argued in [1], observational constraints on the amplitude of string-induced CMB perturbations place limits on  $G\mu/\sqrt{\lambda}$ , where  $\mu$  is the string tension and  $\lambda \leq 1$  is a dimensionless measure of the intercommutation rate. The constraint reported in [1], based on WMAP [14, 15, 16] and 2dF data [17], was  $G\mu \lesssim 1.3 \times 10^{-6} \sqrt{B\lambda/0.1}$ , where  $B$ , defined by Eq. (1), measures the importance of perturbations induced by cosmic strings. It was argued that, conservatively, the currently available data still permit  $B \lesssim 0.1$ . This bound on the parameter  $B$  was found by minimizing the  $\chi^2$  with respect to variations in the parameters  $B$ ,  $W$ , and  $n_s$ , the spectral index of the adiabatic fluctuations power spectrum. The uncertainty in the minimum  $\chi^2$  was translated into an upper bound on  $B$ . This statistical procedure was not rigorous, although the derived bound should be reasonably secure.

In this paper we re-calculate the bound on  $B$ , varying the same parameters as in [1], but using a rigorous Bayesian likelihood analysis. Except for the statistical methods used, and for fitting to the SDSS instead of the 2dFGRS power spectrum, our setup is identical to the one used in [1] and the interested reader can find most of the details there. Here we only mention that  $C_l^{\text{strings}}$  were computed using a modified version [18] of CMBFAST [19] which uses as its active source the energy-momentum tensor components calculated using the local string network model originally suggested in [20] and further improved in [18, 21].  $C_l^{\text{adiabatic}}$  were computed using a recent version of CMBFAST. As in [1], we vary the value of the spectral index  $n_s$ , while holding the following parameters fixed at their best-fit values as determined by WMAP [15]:  $\Omega_m h^2 = 0.14$ ,  $\Omega_b h^2 = 0.024$ ,

$\Omega_\Lambda = 1 - \Omega_m - \Omega_b$ ,  $h = 0.72$ ,  $\tau = 0.166$ . Our rationale is that cosmic strings are only a small correction to the WMAP best-fit. Elsewhere [2], we shall present a more complete study in which we also allow  $\Omega_m h^2$ ,  $\Omega_b h^2$ ,  $\tau$  and  $h$  to vary as well.

According to Bayes's theorem, the posterior distribution for  $W$ ,  $B$  and  $n_s$  is given by

$$P(W, B, n_s | D, M) = \frac{P(W, B, n_s | M) \mathcal{L}(D | W, B, n_s, M)}{P(D | M)}, \quad (2)$$

where  $\mathcal{L}(D | W, B, n_s, M)$  is the likelihood,  $M$  denotes our model and  $D$  stands for data. We use WMAP's CMB temperature anisotropy power spectrum ( $TT$ ) and the temperature-polarization cross-correlation ( $TE$ ) together with the power spectrum ( $P(k)$ ) from the SDSS experiment. For  $TT$  and  $TE$  we have used the likelihood function provided by the WMAP team [16, 22] and for  $P(k)$  the SDSS likelihood code provided by Max Tegmark [23, 24]. The combined  $TT+TE+P(k)$  likelihood is simply the product of individual likelihoods.

We choose flat priors,  $P(W, B, n_s)$  for parameters  $W$ ,  $B$  and  $n_s$  with ranges  $W \in [0.95, 1.05]$ ,  $B \in [0.0, 0.105]$ , and  $n_s \in [0.955, 1.02]$ . We then survey this parameter space using a  $73 \times 65 \times 27$  grid for  $W, B$  and  $n_s$ , respectively. At each grid point we calculate four predicted spectra from our model:  $C_l^{TT}$ ,  $C_l^{TE}$ ,  $C_l^{EE}$ , and  $P(k)$ . The SDSS power spectrum is determined up to an overall bias factor, so the bias has to be included into our analysis as a fourth parameter. The bias and the effect of the spectral distortions on  $P(k)$  can be parametrized via an overall multiplicative factor, which we vary over the range  $[1.50, 1.86]$  – a range large enough to include the maximum likelihood bias value for every grid point – and over which we marginalize. After compiling the full likelihood grid, we marginalize over  $W$  and  $n_s$  separately and plot the resulting likelihood contours. In Figs. 1 and 2 we show the contours in the  $(W, B)$  and  $(n_s, B)$  planes respectively. Finally, we marginalize over both  $W$  and  $n_s$  to find the posterior for  $B$ , shown in Fig. 3. In a similar manner, we have also generated the posteriors for  $W$  (Fig. 4) and  $n_s$  (Fig. 5). The posterior results for  $W$  can be interpreted in light of Fig. 3's results for  $B$ , especially with the help of Fig. 1. We see that there is something of a degeneracy between  $W$  and  $B$ , so that an increase in  $B$  is compensated by a decrease in  $W$ . Nevertheless, our determination,  $W = 0.985 \pm 0.025$ , has a much smaller range than that found by WMAP with  $B = 0$ :  $W = 1.0 \pm 0.11$  [15]. For the spectral index, we find  $n_s = 0.995 \pm 0.0165$ . For comparison, Spergel et al. [15] find  $n_s = 0.99 \pm 0.04$  but vary many more parameters. We note, from Fig. 2, that the approximate  $\Delta \ln(\mathcal{L}) = 1$  range for  $n_s$  is  $\approx 0.995 \pm 0.005$  at  $B = 0$ . We therefore suspect that the relatively narrow range we find for  $n_s$  could broaden when we vary  $\Omega_m$ ,  $\Omega_b$ ,  $\tau$  and  $h$  in addition to  $W$ ,  $B$ , and  $n_s$ .

Our principal result is Fig. 3, the posterior for our cosmic string weighting parameter,  $B$ . We note that, despite our use of the unadjusted WMAP best-fit param-

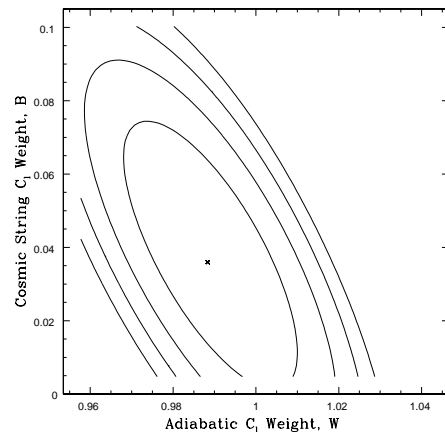


FIG. 1:  $\Delta(\ln(\mathcal{L})) = 1, 2, 3,$  and  $4$  contours after the likelihood grid has been marginalized over  $n_s$ . The maximum likelihood model is marked.

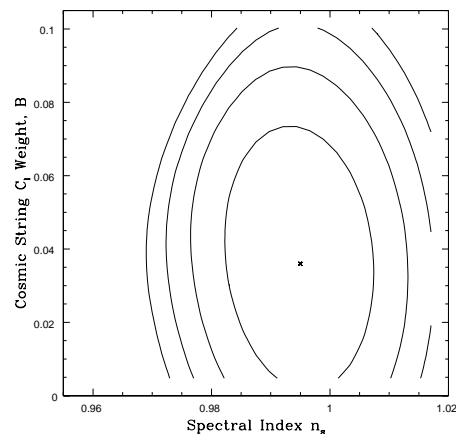


FIG. 2:  $\Delta(\ln(\mathcal{L})) = 1, 2, 3,$  and  $4$  contours after the likelihood grid has been marginalized over  $W$ . The maximum likelihood model is marked.

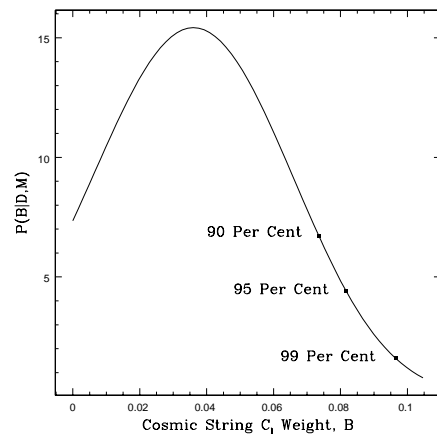


FIG. 3: This plot shows  $P(B|D, M)$  after marginalization over both  $W$  and  $n_s$ . The three dots indicate the regions containing 90, 95, and 99 per cent of the probability, respectively

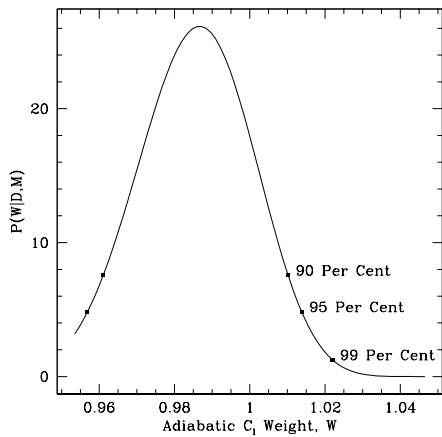


FIG. 4: This plot shows  $P(W|D, M)$  after marginalization over both  $B$  and  $n_s$ . The dots indicate the regions containing 90, 95, and 99 per cent of the probability, respectively

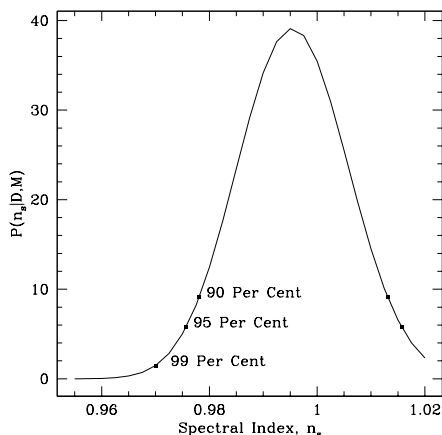


FIG. 5: This plot shows  $P(n_s|D, M)$  after marginalization over both  $W$  and  $B$ . The dots indicate the regions containing 90, 95, and 99 per cent of the probability, respectively

eters for all cosmological factors save  $n_s$ , our additional cosmic string degree of freedom still improves the fit to the data, with the likelihood maximum likelihood falling at  $B \approx 0.04$ . However, at the 90% confidence level, our results are also roughly consistent with  $B = 0$ , while the upper bound at 99% confidence is  $B \lesssim 0.09$ , quite close to what was found much less rigorously in [1]. This upper bound might still permit observable signatures such as pulsar timing [25], gravitational wave bursts [26], and distinctive double lensing events [27]. That the peak for  $B$  is not at zero, however, underscores the necessity of varying the other cosmological parameters,  $\tau$ ,  $h$ ,  $\Omega_m$ , and  $\Omega_b$  as well. We have begun work on this multi-parameter analysis using the Markov Chain Monte Carlo method [2].

#### Acknowledgments

We thank Henry Tye for helpful discussions, Licia Verde for assistance with using the WMAP likelihood code and Max Tegmark for writing an easy to use SDSS likelihood code and making it publicly available [24]. LP would like to thank Ken Olum and Alex Vilenkin for useful conversations. This research is partially supported by NSF Grant No. AST 0307273 (I.W.). M.W is supported by the NSF Graduate Fellowship.

- 
- [1] L. Pogosian, S.-H. Henry Tye, I. Wasserman, M. Wyman, Phys. Rev. **D68**, 023506 (2003) .
  - [2] L. Pogosian, I. Wasserman and M. Wyman, in preparation.
  - [3] L. Kofman, A. Linde and A. A. Starobinsky, Phys. Rev. Lett. **76**, 1011 (1996); I. Tkachev, S. Khlebnikov and L. Kofman, A. Linde, Phys. Lett. **B440**, 262 (1998); C. Contaldi, M. Hindmarsh and J. Magueijo, Phys. Rev. Lett. **82**, 2034 (1999); R. A. Battye and J. Weller, Phys. Rev. **D61**, 043501 (2000). Bouchet, F. R., Peter, P., Riazuelo, A. and Sakellariadou, M., Phys. Rev. **D65**, 21301 (2002)
  - [4] G. Dvali and S.-H.H. Tye, Phys. Lett. **B450** (1999) 72, hep-ph/9812483.
  - [5] N. Jones, H. Stoica and S.-H.H. Tye, JHEP **0207** (2002) 051, hep-th/0203163.
  - [6] S. Sarangi and S.-H.H. Tye, Phys.Lett. B536 (2002) 185, hep-th/0204074.
  - [7] G. Dvali and A. Vilenkin, Phys.Rev. **D67**, 046002 (2003), hep-th/0209217
  - [8] N. Jones, H. Stoica and S.-H.H. Tye, hep-th/0303269.
  - [9] G. Dvali and A. Vilenkin, hep-th/0312007.
  - [10] E. J. Copeland, R. C. Myers, J. Polchinski, hep-th/0312067.
  - [11] C. P. Burgess, M. Majumdar, D. Nolte, F. Quevedo, G. Rajesh and R. J. Zhang, JHEP **0107**, 047 (2001), hep-th/0105204.
  - [12] J. Garcia-Bellido, R. Rabadán and F. Zamora, JHEP **0201** (2002) 036, hep-th/0112147.
  - [13] G. Dvali, Q. Shafi, and S. Solganik, D-Brane Inflation, hep-th/0105203; K. Dasgupta, C. Herdeiro, S. Hirano and R. Kallosh, Phys.Rev. **D65** (2002) 126002, hep-th/0203019.

- [14] C. L. Bennett et al., *Astrophys.J.Suppl.* **148**, 1 (2003), astro-ph/0302207.
- [15] D. N. Spergel et al., *Astrophys.J.Suppl.* **148**, 175 (2003), astro-ph/0302209.
- [16] L. Verde et al., *Astrophys.J.Suppl.* **148**, 195 (2003), astro-ph/0302218.
- [17] W. J. Percival et al., *MNRAS* **327**, 1297 (2001).
- [18] L. Pogosian, and T. Vachaspati, *Phys. Rev. D* **60**, 83504 (1999).
- [19] U. Seljak and M. Zaldarriaga, *Ap. J.* **469**, 437 (1996).
- [20] A. Albrecht, R. A. Battye and J. Robinson, *Phys. Rev. Lett.* **79**, 4736 (1997); *Phys. Rev.* **D59**, 023508 (1999).
- [21] A. Gangui, L. Pogosian and S. Winitzki, *Phys. Rev. D* **64**, 43001 (2001).
- [22] <http://lambda.gsfc.nasa.gov/product/map/>
- [23] M. Tegmark et al., *Ap. J.*, accepted, astro-ph/0310725.
- [24] <http://www.hep.upenn.edu/~max/sdss.html>
- [25] V. M. Kaspi, J. H. Taylor and M. F. Ryba, *Ap. J.*, **428**, 713, (1994);  
A. N. Lommen and D. C. Backer, *Ap. J.*, **562**, 297 (2001), astro-ph/0107470;  
A. N. Lommen, astro-ph/0208572;  
A. H. Jaffe and D. C. Backer, *Ap. J.*, **583**, 616 (2003), astro-ph/0210148.
- [26] T. Damour and A. Vilenkin, *Phys. Rev. D* **64** (2001) 064008, gr-qc/0104026.
- [27] L. L. Cowie and E. M. Hu, *Astrophys. J.*, 318, L33 (1987);  
E. M. Hu, *Astrophys. J.*, 360, L1 (1990);  
M. Sazhin et al., *MNRAS*, **343**, 353 (2003), astro-ph/0302547.